[Perfluorosulfonate Ionomer]/[Mixed Inorganic Oxide] Nanocomposites via Polymer-in Situ Sol-Gel Chemistry

Phoebe L. Shao, K. A. Mauritz,* and R. B. Moore

Department of Polymer Science, University of Southern Mississippi, Hattiesburg, Mississippi 39406-0076

Received August 1, 1994. Revised Manuscript Received October 10, 1994[⊗]

[Mixed-metal oxide]/[Nafion] hybrid films were formulated via in situ sol-gel reactions for tetrabutyl titanate/tetraethoxysilane and for aluminum tri-*sec*-butoxide/tetraethoxysilane alkoxide pairs. Inorganic composition profiles across film thicknesses were investigated via X-ray energy dispersive spectroscopy with an environmental scanning microscope. Mechanical tensile analysis was used to infer inorganic oxide nanophase/Nafion interfacial interactions, as well as interknitting of inorganic oxide nanoparticles. The TiO_2 component within the titaniasilicate-filled hybrids was concentrated in glassy near-surface regions, whereas the SiO_2-Al_2O_3 phase within aluminasilicate-filled hybrids was distributed homogeneously causing mechanical ductility. Investigations of structural topology within the inorganic oxide phases were conducted via IR and NMR spectroscopies.

Introduction

In previous work, Mauritz et al. utilized the polar clusters within perfluorosulfonate ionomer (PFSI) films as nanometers-in-scale containment vessels in which $SiO_{2[1-x/4]}(OH)_x$ structures nucleate and grow via in situ sol-gel reactions for tetraethoxysilane (TEOS).[1-7] The pseudoperiodic array of clusters having average center-to-center spacings of 30-50 Å provided a polymerization template directing the morphology of the resultant dry, solid silicon oxide phase. SO_3H groups in clusters catalyze alkoxide hydrolysis although various cation-exchanged forms are also useful.[8-10] We characterized these unique hybrid materials for structure and properties using electron microscopy, SAXS, WAXD, ^{29}Si solid-state NMR, infrared and dielectric relaxation spectroscopies, DSC, TGA, mechanical tensile, and gas permeation analyses.

This earlier work established the validity of our template hypothesis of in situ inorganic growth. SAXS, WAXD, and DSC studies revealed that the clustered + semicrystalline morphology remains intact despite invasion by the silicon oxide component up to moderate filler levels.[4-6] Mechanical tensile tests, especially, indicated a percolation of the silicon oxide phase with increasing filler content,[1] and IR and ^{29}Si NMR spectroscopies[1,2,8] provided insight into molecular connectivity within the fractal-like silicon oxide phase. Recently, we formulated and characterized similar but more complex hybrids in which organic "shells" were constructed about preformed $SiO_{2[1-x/4]}(OH)_x$ nanostructures via postreactions of ethoxymethylsilanes with Si-OH groups on nanoparticles.[11] On the basis of the success of these earlier efforts, we are synthesizing [inorganic oxide]/PFSI nanocomposites having greater compositional and structural complexity. The component of this work reported here deals with mixed metal oxide nanophases.

A formidable quantity of papers dealing with formulation strategies and characterization of multicomponent gels issuing from solutions of mainly Si, Ti, Al, Zr, and B alkoxide combinations via the sol-gel route have appeared, many in the *Journal of Noncrystalline Solids*, during the past decade and a half. A few useful collections of monographs, beginning with that edited by Hench and Ulrich, discuss multicomponent gels.[12] We found that studies involving compositions of interest to our work, namely, SiO_2-TiO_2 and SiO_2-Al_2O_3, were of limited use in guiding our experiments for the following reasons. First, the end products result from heating gels to temperatures well beyond those to which our hybrids would be subjected and above that at which Nafion degrades (slightly above 340 °C). Second, the samples are often monolithic, possessing macroscopic dimensions, whereas in our work the inorganic oxide phases are highly dispersed, possessing high surface/volume, and are often constrained to small geometries (nanometers-in-size polar clusters) within a perfluorosulfonate ionomer. We have cited herein references containing important IR and NMR spectroscopic band assignments for sol-gel-derived SiO_2-TiO_2 and SiO_2-Al_2O_3 glasses.

[⊗] Abstract published in *Advance ACS Abstracts*, November 15, 1994.

(1) Mauritz, K. A.; Storey, R. F.; Jones, C. K. in *Multiphase Polymer Materials: Blends, Ionomers and Interpenetrating Networks*; ACS Symp. Ser. No. 395, Ch. 16; Utracki, L. A., Weiss, R. A., Eds.; American Chemical Society: Washington, DC, 1989.

(2) Mauritz, K. A.; Warren, R. M. *Macromolecules* **1989**, *22*, 1730.

(3) Mauritz, K. A.; Stefanithis, I. D. *Macromolecules* **1990**, *23*, 1380.

(4) Stefanithis, I. D.; Mauritz, K. A. *Macromolecules* **1990**, *23*, 2397.

(5) Mauritz, K. A.; Stefanithis, I. D.; Wilkes, G. L; Huang, Hao-Hsin *ACS Div. Polym. Chem., Polym. Prepr.* **1991**, *32* (1), 236.

(6) Mauritz, K. A.; Stefanithis, I. D.; Wilkes, G. L; Huang, H.-H. *J. Appl. Polym. Sci.*, in press.

(7) Mauritz, K. A; Scheetz, R. W.; Pope, R. K.; Stefanithis, I. D. *ACS Div. Polym. Chem., Polym. Prepr.* **1991**, *32* (3), 528.

(8) Davis, S. V.; Mauritz, K. A. *Am. Chem. Soc., Polym. Prepr.* **1992**, *33* (2), 363.

(9) Davis, S. V.; Mauritz, K. A. *Am. Chem. Soc., Polym. Prepr.* **1993**, *34* (1), 608.

(10) Bordayo, C.; Davis, S. V.; Moore, R. B.; Mauritz, K. A. *Am. Chem. Soc. PMSE Div. Prepr.* **1994**, *70*, 230.

(11) Deng, Q.; Mauritz, K. A. In *Hybrid Organic-Inorganic Composites, ACS Symp. Ser.*; Mark, J. E., Bianconi, P. A., Lee, Y.-C., Eds., in press.

(12) (a) Hench, L. L., Ulrich, D. R., Eds. *Ultrastructure Processing of Ceramics, Glasses, and Composites*; John Wiley & Sons: New York, 1984. (b) Hench, L. L., Ulrich, D. R., Eds. *Science of Ceramic Chemical Processing*; John Wiley & Sons: New York, 1986.

0897-4756/95/2807-0192$09.00/0

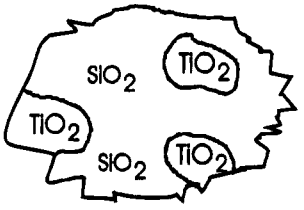

Figure 1. Rough depiction of silicon oxide–metal oxide composition segregation within nanoparticles grown within the polar clusters of PFSI templates. Within each domain the other component might exist in dilute concentration.

The alkoxides utilized were TEOS in combination with the more rapidly reacting metal (M) alkoxides Ti(OR)$_4$ and Al(OR)$_3$. Although these alkoxides can be mixed on a molecular level in macroscopic alcohol solutions, the possibility exists for ultimate *compositional segregation* within nanoparticles grown within the polar clusters of dried–annealed films owing to considerable differences between hydrolysis–condensation rates for Si and M alkoxides, as illustrated in Figure 1. Moreover, two inorganic alkoxides of different size, shape, and outer groups are expected to have different permeation rates within the PFSI template. Different degrees of Si–M oxide molecular interconnectivity were anticipated and investigated using IR and ^{29}Si solid-state NMR spectroscopies. Different Si/M ratios will generate varying degrees of intraparticle molecular connectivity, which will influence the convoluted intraparticle free volume. Perhaps [perfluoroorganic]/[inorganic oxide] interfaces having different fractal dimensions or "roughness" can be tailored in this way.

Another important structural aspect, but on a larger scale, is the geometrical distribution of the inorganic phase throughout the PFSI template. In consideration of relative rates of permeation and reaction for different alkoxide species and the simple fact that the outer, near-surface regions of the PFSI sample will be exposed to the alkoxide diffusants at an earlier time than the inner regions, it is reasonable to expect that the resultant distribution of the solid inorganic oxide phase across the film thickness direction will be nonuniform. We will directly examine these compositional profiles using the X-ray energy-dispersive spectroscopy attachment (EDS) of an environmental scanning microscope (ESEM).

The specific goals and methods of the work in this report were: (1) To create [mixed-metal oxide]/PFSI hybrids via in situ sol–gel reactions for sorbed, premixed Ti–Si and Al–Si alkoxide pairs; (2) to investigate inorganic composition profiles across the film thickness directions of these materials via ESEM/EDS; (3) to infer, by mechanical tensile analysis, inorganic nanophase/PFSI interfacial interactions, as well as the possible interknitting of inorganic oxide nanoparticles; (4) to present limited results of our investigation of short-range structure within the inorganic oxide phase using IR and NMR spectroscopies.

Variation of compositional contrast either on the level of nanometers or on the larger scale spanning the dimensions of the sample is expected to have important implications regarding the mechanical, thermal, optical, dielectric, diffusion, and electrical transport properties of these hybrids in the forms of films, membranes, coatings, or fibers.

Table 1. TEOS/TBT Initial Solution Composition, Percent Inorganic Oxide Mass Uptake, and Internal Overall Ti/Si EDS Intensity Ratios

mL of TEOS/mL of TBT/mL of 2-propanol	% mass uptake	Ti/Si
15/5/40	7.60	9.61
10/10/40	7.06	13.45
5/15/40	6.56	23.31
0/20/40	6.42	

These heterogeneous materials are expected to interact strongly and specifically with electromagnetic fields owing to gradients of dielectric permittivity and charge conductivity across the nanophase boundaries. As phase separation exists on a scale considerably smaller than wavelengths in the optical region, light will not be scattered. Index of refraction in similar hybrids can be tailored by manipulating alkoxide mixture composition. An asymmetric distribution of the inorganic oxide component, say across a film or coating thickness direction or perpendicular to the axis of a fiber, would generate a distribution of index of refraction that might be useful in tailoring waveguide properties. It might also be worthwhile to consider the inorganic oxide phase of these hybrids as platforms onto which noncentrosymmetric molecules having a nonlinear optical response can be attached. For the latter, the sol–gel process in the presence of NLO molecules, could be conducted under electrical poling, as described by Nosaka et al.[13]

Experimental Procedure

Sorption of Premixed Alkoxides: [SiO_2–TiO_2 (mixed)]/Nafion Nanocomposites. The PFSI morphological templates were 1100 equivalent weight, 5 mil-thick, H^+-form Nafion membranes. Samples were placed in boiling water for 30–60 min and then mildly dried at 50 °C for 4 h to remove loosely bound water. We do not know the exact amount of incorporated water at this stage, but the procedure was conducted in precisely the same fashion within a given series of experiments to ensure sample reproducibility. Then, the sparsely-hydrated membranes were swollen in 2-propanol for 1 h to promote subsequent permeation of inorganic alkoxides.

TEOS and tetrabutoxy titanate (TBT) were premixed with various compositions in 2-propanol. Afterward, all alcohol-swollen membranes were immersed in the mixed alkoxide solutions for 30 min and then removed, and the surfaces rinsed with fresh 2-PrOH to minimize precipitation of a surface-attached silica–titania layer, such as we have seen in earlier studies.[6,7,8,14] Samples were then placed in a 100% humidity environment for 10 h to further encourage hydrolysis in slow fashion. Large quantities of water were not introduced at a single time for the purpose of slowing the sol–gel reaction, given that TBT is known to react rapidly. Finally, all samples were vacuum dried at 100 °C for 24 h.

The initial mixed alkoxide solution compositions and resultant dried percent mass uptakes in these experiments are listed in Table 1. All net uptakes do not greatly differ from 7%, although the average Ti/Si intensity ratio increases with increasing TBT solution concentration, as expected.

Sorption of Premixed Alkoxides: [SiO_2–Al_2O_3 (mixed)]/Nafion Nanocomposites. The following sample preparative sequence, as well as the reasons for performing each step, is essentially identical to that given above.

All Nafion-H^+ films were placed in boiling water for 30–60 min and then mildly dried at 50 °C for 4 h. Afterward, the

(13) Nosaka, Y.; Tohriiwa, N.; Kobayashi, T.; Fujii, N. *Chem. Mater.* **1993**, *5*, 930.
(14) Davis, S. V.; Mauritz, K. A.; Moore, R. B. *Am. Chem. Soc., Polym. Prepr.* **1994**, *35* (1), 419.

Table 2. TEOS/ATB Initial Solution Composition, Percent Inorganic Oxide Mass Uptake, and Internal Overall Al/Si EDS Intensity Ratios

mL of TEOS/mL of ATB/mL of 2-propanol	% mass uptake	Al/Si
40/2/10	6.50	0.189
80/5/20	4.66	0.328
80/10/20	5.73	0.678
80/20/40	4.68	1.103

samples were swollen in 2-PrOH for 1 h. TEOS and tri-*sec*-butoxyaluminum (ATB) were premixed with various compositions in 2-PrOH solutions. Following this, the alcohol-swollen films were immersed in the mixed alkoxide solutions for 1 h and then removed, and their surfaces were rinsed with fresh 2-PrOH. Experimental steps involving alkoxides were performed in a drybox. Samples were then placed in air for about 10 h. As before, all samples were vacuum-dried at 100 °C for 24 h.

Precursor alkoxide-alcohol solution compositions, final dried inorganic oxide weight uptakes, and average internal Al/Si ratios obtained by SEM-EDS analysis, are listed in Table 2. Percent uptake does not show a trend with composition and is somewhat low, particularly in the sense of being below the percolation threshold for this phase. These uptakes do not differ greatly from those of the SiO_2–TiO_2 filled system. These facts will be important in the analysis of stress vs strain profiles. Average internal Al/Si ratio increases with decreasing solution TEOS/ATB ratio, as is reasonable.

Inorganic Oxide Concentration Profiles across Film Thickness Direction. An environmental scanning electron microscope (Electroscan ESEM) was used to study large-scale morphologies of these nanocomposites. We present examples of our use of the X-ray energy dispersive elemental microprobe attachment of the ESEM/EDS to determine Si, Ti, and Al elemental profiles across sample thicknesses.

The ESEM, as well as an optical microscope, was also used to determine if an undesirable glassy inorganic oxide layer precipitated on the surfaces of films during nanocomposite formation. Not only would this layer, referred to earlier, present an undesirable complication from the standpoint of materials applications but also structure–properties data (particularly FT-IR/ATR spectra) intended to be representative of the bulk would be distorted, at best. We simply mention that microscopic inspection of the surfaces of samples in this study did not reveal such a layer.

The integrated intensity of the sulfur (S) peak in the X-ray energy spectrum quantifies SO_3^- group population within a selected area and is adopted as a reference for the polymer matrix. Therefore, for example, Si/S intensity ratio is a relative measure of local silicon oxide content.

An inorganic oxide compositional gradient is rationalized in the following way: Owing to diffusion limitation, the outer regions of the PFSI will be exposed to the in-migrating alkoxide molecules at an earlier time than the inner regions. Moreover, alkoxide molecules will diffuse to the middle of the films with progressive difficulty due to the obstacles posed by already-precipitated inorganic structures in near-surface regions.

Mechanical Tensile Measurements. Stress vs strain tests were performed at 22 °C using an MTS 810 Universal Test Machine at a strain rate of 0.1 mm/s on 3 mm wide × 1 cm long samples.

Infrared Spectroscopic Investigation. FT-IR/ATR spectra were obtained using a Bruker 88 spectrometer at a resolution of 4 cm^{-1}. A thallium bromide–thallium iodide (KRS-5) crystal was used as the ATR plate with an angle of incidence of 45°. A total of 1000 interferograms was taken in each case.

As in our earlier similar IR investigations of these hybrids, the reflectance mode must be used because of the high absorbance associated with these thicknesses.[1,2] Therefore, the interpretation of FT-IR/ATR spectra for these hybrids should take into account the results of our parallel ESEM/EDS investigations with regard to whether the inorganic oxide component is distributed uniformly across the film thickness or highly concentrated near the surfaces. For the latter case, the spectra cannot be considered as being representative of the bulk.

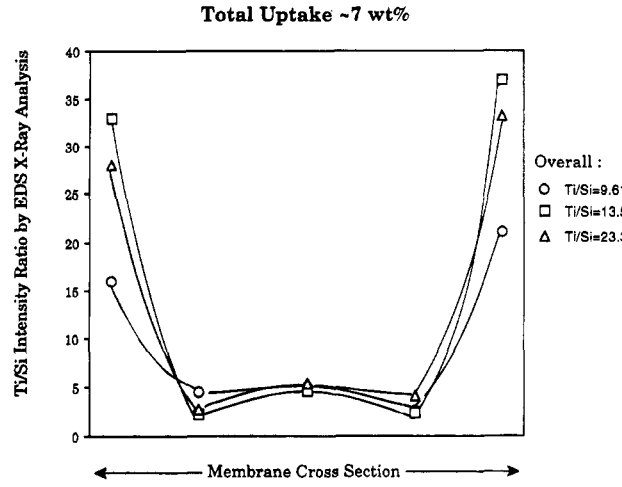

Figure 2. Typical Ti/Si composition profiles across the PFSI film thickness, for the average Ti/Si ratios listed in Table 1, and labeled to the right of the figure. The left and right end points of the horizontal axis correspond to the film surfaces.

^{29}Si Solid-State NMR Spectroscopy. The NMR spectrum for a selected SiO_2–Al_2O_3/Nafion hybrid was obtained on a Bruker MSL-400 spectrometer operating at a frequency of 79.5 MHz for the silicon nucleus. A standard CP/MAS probe was used to acquire solid-state spectra. Samples were packed in fused zirconia rotors equipped with Kel-F caps, and the sample spinning rate was 5.4 kHz. Spectra were acquired using high-power decoupling during acquisition only. Cross-polarization was not possible due to the paucity of protons in the samples. The 90° pulse width was 5.2 μs, and a relaxation delay of 10 s was used. The number of scans was 15 409. All chemical shifts were in reference to the downfield peak of tetrakis(trimethylsilyl)silane (−9.8 ppm with respect to TMS). The experiment was performed at 22 °C.

Results: SiO_2–TiO_2-Filled Systems

ESEM/EDS Studies. Figure 2 shows three typical composition profiles, each for the average Ti/Si ratio (i.e., for a large area of the cross section extending from film surface-to-surface) in Table 1 and listed to the right of the figure. The curves are rather symmetrical about the film center plane. The Ti/Si ratio is the greatest and increases with increasing $(Ti/Si)_{average}$ in the near-surface regions. We attribute the large relative concentration of TiO_2 in the immediate subsurface regions, as well as the sharp negative gradient of this quantity toward the center, to the high TBT sol–gel reaction rate compared to the rate of inward TBT diffusion and slow TEOS sol–gel reaction rate.

Figure 3, which depicts the Ti/S ratio for the same system, shows that in absolute terms, i.e., scaled to the number of SO_3H groups, there is more TiO_2 near the surface than at any other location, especially the middle.

Mechanical Tensile Studies. Corresponding stress vs strain curves (Figure 4) show that the pure SiO_2-containing PFSI is ductile in the same way as for the unfilled PFSI as seen in earlier studies.[1,9] This is reflective of a situation where filler is beneath its percolation threshold uptake. Therefore, the ionomer

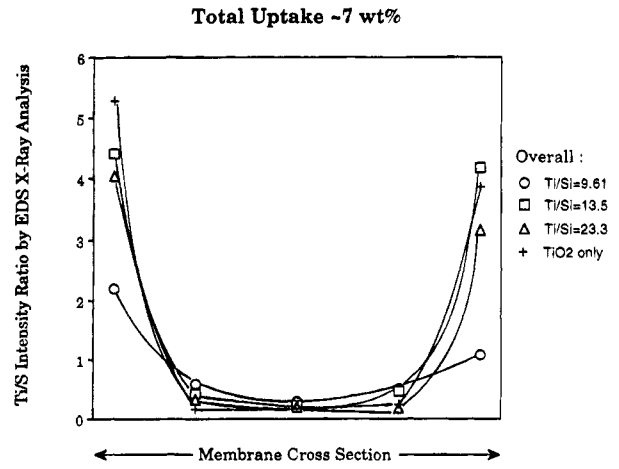

Figure 3. Typical Ti/S composition profiles for the average Ti/Si ratios in Table 1, and labeled to the right of the figure. The left and right end points of the horizontal axis correspond to the film surfaces.

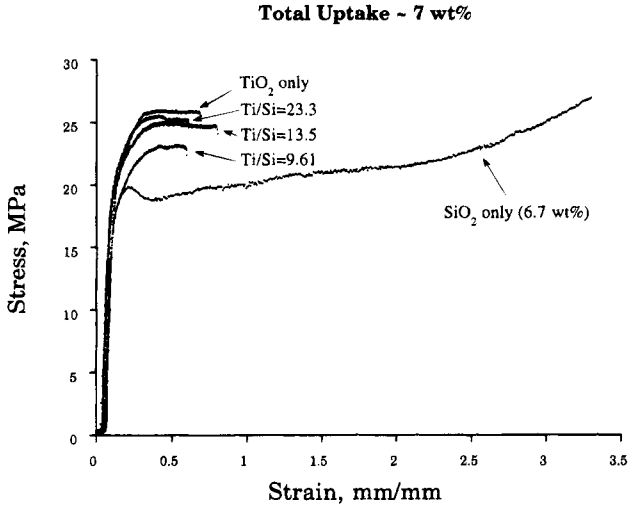

Figure 4. Tensile stress vs strain profiles for [mixed TiO_2–SiO_2]/Nafion hybrids having indicated inorganic oxide compositions and roughly the same net uptake.

template would seem to be the load-bearing phase in this case.

In sharp contrast, mixed incorporation of TiO_2 renders the material comparatively brittle, suggesting that the inorganic nanoparticles are contiguous over large distances, that is, have a significant degree of interconnection. Interestingly, elongation-to-break is about the same for all mixed compositions and tensile strength monotonically increases with increasing Ti/Si ratio. Given the fact, issuing from the ESEM/EDS studies discussed above, that most of the TiO_2 in these brittle samples resides near the surface, it would seem that this glassy zone, depicted in Figure 5, controls the mechanical properties of these nanocomposites. These results suggest that there is a gradient of ultimate mechanical properties along the film thickness direction so that a hypothetical lamina through the middle of the film, parallel to the surfaces, might in fact be ductile.

FT-IR/ATR and ^{29}Si Solid-State NMR Studies. Owing to the great film depth dependence of the SiO_2–TiO_2 composition revealed by the above ESEM/EDS studies, FT-IR/ATR spectra will not represent a bulk average and, oppositely, NMR spectra will not focus on the importance of the near-surface regions. In future

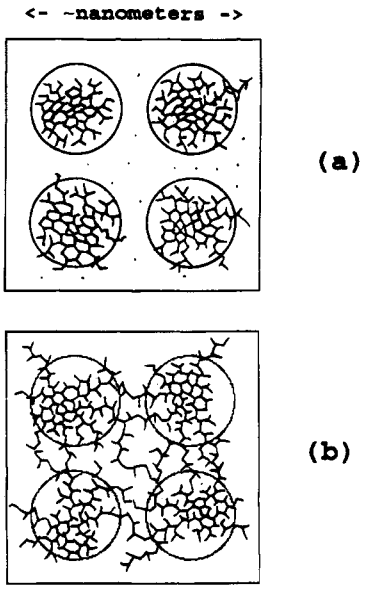

Figure 5. (a) Isolated, cluster-contained inorganic oxide nanoparticles. Only the PFSI phase is continuous. (b) Suggested nanostructure in near-surface glassy zone: inorganic oxide nanoparticles that are interknitted via –Ti–O– chains. PFSI and inorganic oxide phases are co-continuous in this zone.

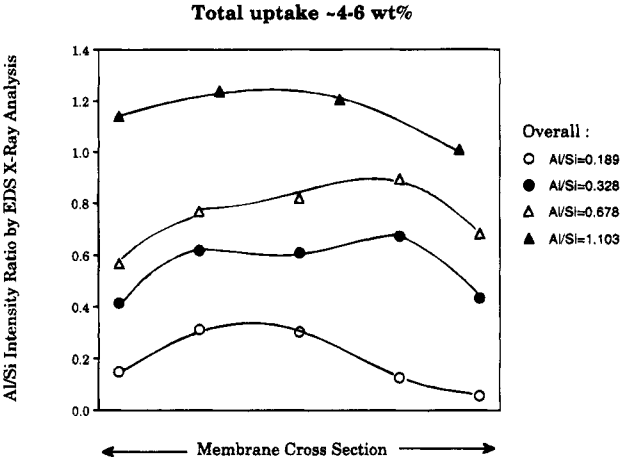

Figure 6. Typical Al/Si composition profiles across the PFSI film thickness, for the average Al/Si ratios listed in Table 2, and labeled to the right of the figure. The left and right end points of the horizontal axis correspond to the film surfaces.

studies, we will attempt to elucidate near-surface vs interior spectral differences and the results reported in a paper dedicated to TiO_2-containing hybrids.

Results: SiO_2–Al_2O_3-Filled Systems

ESEM/EDS Studies. As seen in Figure 6, the Al/Si ratio is relatively uniform, considering the expanded scale on the vertical axis, across the film thickness for all $(Al/Si)_{average}$. This result stands in sharp contrast with the above-observed situation for the [TiO_2–SiO_2]/Nafion hybrids whose composition profiles displayed sharp gradients. In fact, there is actually less Al relative to Si in the near-surface regions. As expected, the curves are displaced upward with increasing $(Al/Si)_{average}$. Figure 7 shows that Al, in an absolute sense (i.e., relative to the internal sulfur standard), can be rather homogeneously distributed across the thickness

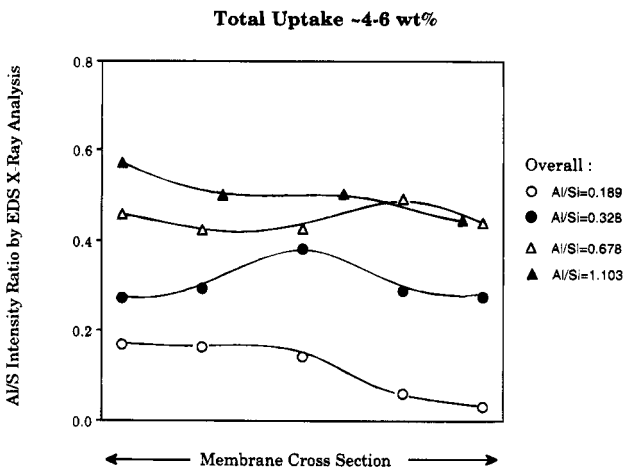

Figure 7. Typical Al/S composition profiles across the PFSI film thickness, for the average Al/Si ratios listed in Table 2, and labeled to the right of the figure. The left and right end points of the horizontal axis correspond to the film surfaces.

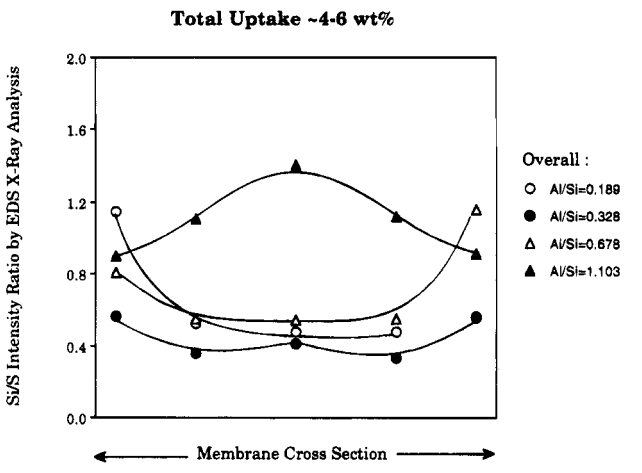

Figure 8. Typical Si/S composition profiles across the PFSI film thickness, for the average Al/Si ratios listed in Table 2, and labeled to the right of the figure. The left and right end points of the horizontal axis correspond to the film surfaces.

direction. It is quite interesting that for Al/Si = 0.328, the greatest concentration of Al is in the middle. Apparently, ATB molecules have the ability to penetrate deep into the film before they polymerize to sizes at which they are no longer mobile. As ATB is fast-reacting, the cause of this result may be a high diffusivity for this alkoxide within the PFSI morphology. Of course, this explanation exists within the realm of speculation, as diffusion in this context is not "simple" but coupled to other events within the membrane. Other factors of direct relevance are an evolving sol–gel reaction within the medium that is consuming the reactive diffusant, consuming and generating water, generating additional alcohol, and changing the degree of membrane swelling. Moreover, the consequence of the transesterification and exchange reactions that can take place during the preparation of the multicomponent solutions prior to the uptake of alkoxides may be significant:

$$\mathrm{Si(OEt)_4 + Al(OBu)_3 \rightleftarrows Si(OEt)_{4-x}(OBu)_x + Al(OBu)_{3-x}(OEt)_x}$$

$$\mathrm{Al(OBu)_3 + xPrOH \rightleftarrows Al(OBu)_{3-x}(OPr)_x + xBuOH}$$

There is a range of properties within this broader range of reactive species that are imagined to permeate the PFSI film, especially with regard to differences between hydrolysis rates of the different Al alkoxide possibilities. It was suggested in the review of this paper that this prepermeation chemistry might in fact explain why the SiO_2–Al_2O_3 is distributed homogeneously.

In Figure 8 it is seen that there can actually be more Si in the middle than near the film surfaces for the hybrid having the highest $(Al/Si)_{average}$.

A general conclusion, upon comparing the Ti- with the Al-containing hybrids formulated in this way, is that the composition profiles are drastically different. This factor, in turn, is seen to influence mechanical properties in a profound way.

Mechanical Tensile Studies. As seen in Figure 9, stress vs strain curves for all [SiO_2–Al_2O_3]/Nafion hybrids portray ductility but less elongation-to-break than pure SiO_2-filled Nafion. We suggest that the

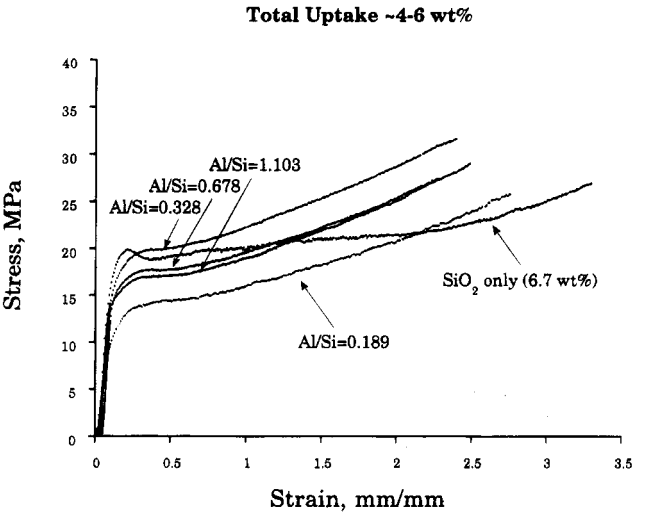

Figure 9. Tensile stress vs strain profiles for [mixed Al_2O_3–SiO_2]/Nafion hybrids having indicated inorganic oxide compositions and roughly the same net uptake.

relatively homogeneous distribution of the inorganic oxide phase, as discussed in the previous section, is a condition under which the percolation of this phase is impossible throughout any hypothetical lamina parallel to the film surfaces. To be sure, the condition portrayed in Figure 5b, with the implication of glassy near-surface layers, does not exist in this case. Thus, the intrinsically ductile PFSI matrix always appears to be the load-bearing phase for the samples in this particular set of formulations, although the situation for greater uptakes may be different.

All hybrids appear, on inspection, to have about the same Young's modulus. Except for the hybrid having the lowest ratio (0.189), tensile strength decreases while elongation-to-break remains approximately the same with increasing $(Al/Si)_{average}$.

FT-IR/ATR Studies. Figure 10 shows difference spectra (i.e., [SiO_2–Al_2O_3/Nafion] spectrum − [unfilled dry Nafion-H^+] spectrum) for samples having the indicated Al/Si ratios derived from ESEM/EDS analysis. Analysis of the inorganic phase of these hybrids by inspecting the total IR spectrum is difficult because of the presence of the numerous and complex bands

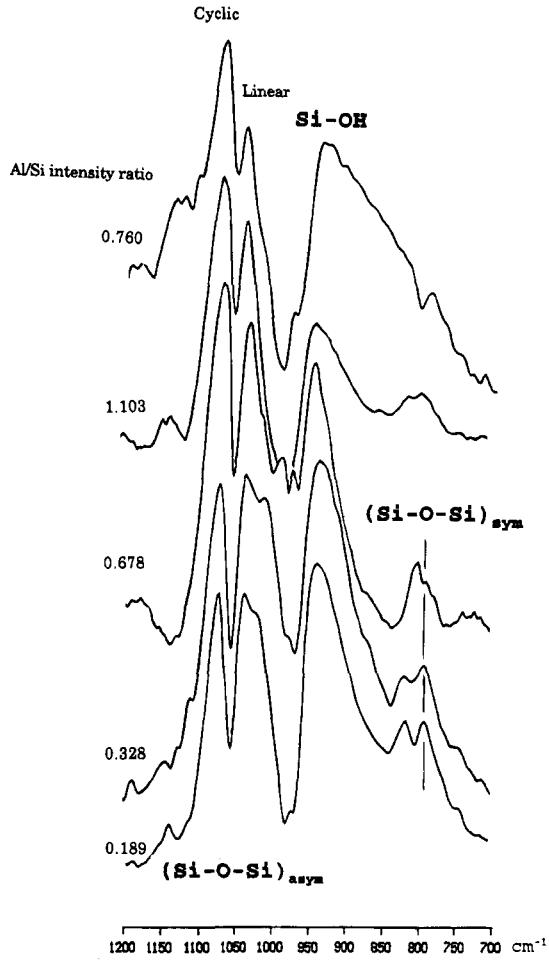

Figure 10. FT-IR/ATR difference spectra (Al_2O_3–SiO_2/Nafion–unfilled dry Nafion-H^+) from 1200 to 700 cm^{-1}, for hybrids of various Al/Si ratios, with major silicon oxide peaks labeled.

characteristic of pure Nafion.[15] Therefore, subtraction of the spectrum of the unfilled dry Nafion-H^+ film precursor from that of the hybrid is necessary to study the structure of the incorporated alumina/silica phase in this way. Figure 10 focuses on the spectra over the range 1200–700 cm^{-1}, a region containing important vibrations of Si–O–Si and SiOH groups.

The spectral subtractions were successful in uncovering major peaks characteristic of molecular groups in the mixed inorganic oxide phase. For one, the observed Si–O–Si asymmetric stretching vibration (~1000–1100 cm^{-1}) is the signature of bridging oxygens, that is, of completed condensation reactions. This characteristic vibration is actually split into two components arising from groups in linear and cyclic configurations as discussed previously.[2] Comparison of the integrated intensities of the linear and cyclic components contributes to understanding the degree of molecular connectivity within the inorganic oxide phase.

Also, the absorbance associated with Si–OH vibration (~940 cm^{-1}) is a measure of degree of hydrolysis or of the relative number of uncondensed silanol groups. The (integrated) intensity ratio $I_{\upsilon(SiOH)}/I_{\upsilon(Si-O-Si)asym}$ would measure the degree of cross-linking within a silicon oxide phase if the aluminum oxide component were not

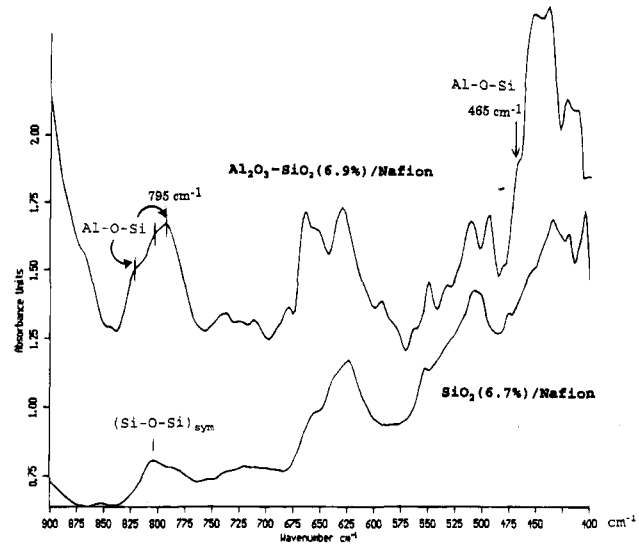

Figure 11. FT-IR/ATR difference spectra, as before, but from 900 to 400 cm^{-1} for the following two hybrids: (1) SiO_2 (6.7%)/Nafion and (2) $SiAl_2O_5$ (6.9%)/Nafion for which the Al:Si mole ratio in the external alkoxide solution was 1:9.

inserted into the structure. In this work, we will note trends in these spectral features on a qualitative basis.

The spectra in Figure 10 portray a progressive increase of Si–O–Si groups in loops, as opposed to linear fragments, with increase in Al/Si ratio. Actually, the ratio of the cyclic-to-linear peak absorbance is a maximum for this series for Si/Al = 0.760. The region of the "linear" Si–O–Si peak actually consists of two overlapping peaks where the low-frequency component decreases in relative intensity with increasing Al/Si ratio. We presently do not understand the origin of these companion peaks. A structure such as a loop or a chain must contain a sufficiently large number of consecutive Si–O groups, perhaps more than four. Evidence that such structures exist suggest that Si/Al compositional segregation exists, although more direct evidence is needed for clarity. Concurrently, Si–OH group absorbance decreases, although this may simply reflect a lower Si/Al ratio.

Figure 11 consists of spectra, in the low wavenumber region, for the following two hybrids: (1) SiO_2 (6.7%)/Nafion and (2) SiO_2–Al_2O_3 (6.9%)/Nafion for which the Al:Si mole ratio in the external alkoxide solution was 1:9. Comparison between the two spectra is meaningful as both samples have nearly the same inorganic oxide uptake.

In both spectra, an absorption in the region of the symmetric vibration of the Si–O–Si group is present. As discussed in an earlier report, this mode is theoretically infrared-inactive but present owing to distortion from coordinative symmetry of bonding about the SiO_4 tetrahedra.[2] In fact, we have also seen (unpublished) this band in Raman spectra of SiO_2/Nafion hybrids at the same wavenumber. This IR peak appears rather unambiguously at ~800 cm^{-1} for system 1. On the other hand, two bands appear on either side of this peak for system 2. This fact is in harmony with the results of Edney et al., who interpreted infrared spectra of SiO_2–Al_2O_3 glasses prepared by the sol–gel process.[16]

(15) Falk, M. In *Perfluorinated Ionomer Membranes, ACS Symp. Ser. 180*; Eisenberg, A., Yeager, H. L., Eds.; American Chemical Society: Washington, DC; p 139.

(16) Edney, C. V.; Condrate, R. A.; Crandall, W. B. *Mater. Lett.* **1987**, *5*, 463.

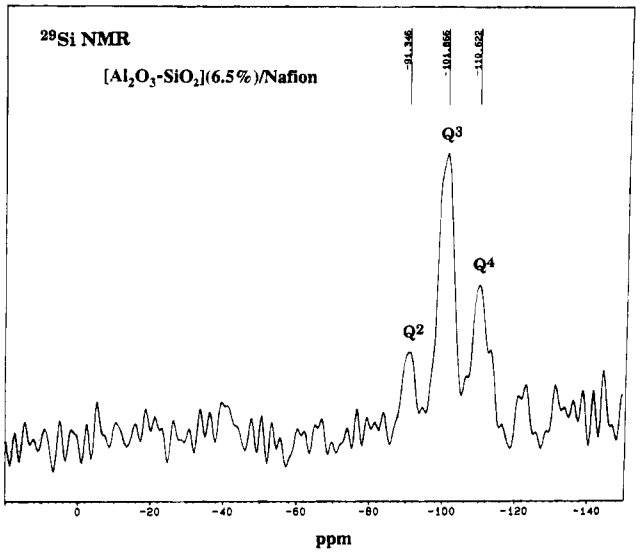

Figure 12. ^{29}Si solid-state NMR spectrum for a $SiAl_2O_5$ (6.5%)/Nafion hybrid, having Al/Si ~ 0.19. While Q^2, Q^3, and Q^4 regions are labeled, $Q^4(m\text{Al})$ possibilities also exist.

In this work, these bands were interpreted as being perturbations of silicate modes caused by the presence of four-coordinated aluminum atoms and/or Al-O-Si linkages within the glass network.

An absorption around 450 cm^{-1} in pure SiO_2-containing systems has been associated with either Si−O−Si bending or rocking vibration.[2] The width of this peak should reflect the distribution of Si−O−Si bond angles. This distribution is imagined to be broad for system 1 but even broader for the more complicated system 2. While we are unaware of relevant model studies, it is reasonable to think that the following numerous Si−O−Si group nearest-neighbor substitution possibilities contributes to the broadening of bands involving this group or might even cause band splitting:

$$(HO)_{4-x-y}(SiO)_x(AlO)_y[Si-O-Si](SiO)_n(AlO)_m(OH)_{4-n-m}$$

Another signature of the Si−O−Al bond cited by Edney et al. and seen in Figure 11, is the high frequency shoulder, at 465 cm^{-1}. Although these studies are in an exploratory stage, it appears that IR spectroscopy can probe degree of inorganic oxide molecular network connectivity at least on a short-range basis.

^{29}Si Solid-State NMR Study. Figure 12 shows a ^{29}Si CP-MAS NMR spectrum for a $SiAl_2O_5$/Nafion hybrid (dry inorganic oxide content = 6.5%), reacted with premixed alkoxides having Al/Si ~ 0.19. The ^{29}Si and ^{27}Al NMR studies, of Yasumori et al.,[17] of sol−gel-derived Al_2O_3−SiO_2 glasses are relevant in the interpretation of the spectra of the PFSI-in situ-grown aluminsilicate phases in this work. In a *pure* silicate, SiO_4 tetrahedra can exist in five states of coordination involving Si−O−Si bonds, each state designated by the symbol Q^n, n being the degree of Si atom substitution. The approximate chemical shift (ppm, relative to Si(Me)$_4$) ranges of Q^n are listed in Table 3.[18] Yasumori et al. point out that in aluminasilicates the SiO_4 tetrahedra with four bridging oxygens are classifed into five species according to the number of adjacent Al atoms, m, bonded to the oxygen: $Q^4(m\text{Al})$, i.e. $Si(OSi)_{4-m}(OAl)_m$. The approximate ranges of the chemical shift of $Q^4(m\text{Al})$ are indicated in Table 3.[17]

Table 3. Chemical Shift (ppm) Ranges for $Q^4(m\text{Al})$ and Q^n Species

Al substitution	chemical shift	Si substitution	chemical shift
Q^4(4Al)	−81 to −91	Q^0	−60 to −82
Q^4(3Al)	−85 to −94	Q^1	−68 to −83
Q^4(2Al)	−91 to −100	Q^2	−74 to −93
Q^4(1Al)	−97 to −107	Q^3	−91 to −101
Q^4(0Al)	−101 to −116	Q^4	−106 to −120

It is seen, on inspection of Table 3, that there is considerable overlap between the $Q^4(m\text{Al})$ and Q^n peak ranges so as to confuse the assignments of the peaks observed at ca. −91, −102, and −111 ppm in Figure 12. This fact, coupled with the high noise/signal in the spectrum, adds ambiguity to assignment of peaks to definite states of coordination and we feel that we can only comment on the distribution of chemical shifts about the three observed peaks in the most general terms.

With reference to Table 3, the resonance at −91 ppm, the least intense of the three, falls within ranges corresponding to the following coordinations: $(SiO)_2Si(OH)_2$ and $(SiO)Si(OAl)_3$. There is no indication from the spectrum that just one or the other or both groups is/are present. The resonance at −102 ppm, the strongest, likewise corresponds most closely to $(SiO)_3SiOH$ and $(SiO)_3SiOAl$ fragments, and the −111 ppm peak quite definitely to $(SiO)_4Si$. This structural distribution reflects, in a general way, the fact that Si exists in higher concentration than Al (Table 2). The IR spectrum for this sample (Figure 10) indicates a large relative number of SiOH groups. This fact, combined with the fact of higher concentration of Si relative to Al, might favor dominance of the $(SiO)_2Si(OH)_2$ over the $(SiO)Si(OAl)_3$ fragment as responsible for the −91 ppm resonance, as well as dominance of the $(SiO)_3SiOH$ over the $(SiO)_3SiOAl$ structure for the −102 ppm peak region.

There are no IR bands identifying Al−O−Al groups existing in loops or in linear fragments, similar to those for Si−O−Si groups, that we are aware of. Also, the issue of inorganic compositional segregation (i.e., Si-rich or Al-rich regions) is not resolved by these spectroscopic results. Perhaps the presence of the two overlapping IR peaks, rather than the commonly observed singlet for pure SiO_2-filled Nafion, in the region of the "linear" Si−O−Si peak (Figure 10), as well as their shifting in relative absorbance with Al/Si ratio, reflects insertion of Al−O bonds into the silicate structure. Recall that the above IR studies revealed the presence of Si−O−Al groups, indicating that $Q^4(m\text{Al})$, $m > 0$, structures should exist.

General Conclusions

Restating, the goals of this work were (1) to create [mixed-metal oxide]/PFSI hybrids via in situ sol−gel reactions for the sorbed, premixed alkoxide pairs: tetrabutyl titanate/tetraethoxysilane and aluminum tri-*sec*-butoxide/tetraethoxysilane; (2) to investigate inorganic composition profiles across the film thickness

(17) Yasumori, A.; Iwasaki, M.; Kawazoe, H.; Yamane, M.; Nakamura, Y. *Phys. Chem. Glasses* **1990**, *31* (1), 1.
(18) Engelhardt, G.; Michel, D. *High Resolution Solid State NMR of Silicate and Zeolites*; Wiley: New York, 1987.

directions of these materials via ESEM/EDS; (3) to infer, by mechanical tensile analysis, inorganic oxide nanophase/PFSI interfacial interactions, as well as possible interknitting of inorganic oxide nanoparticles; (4) to present limited results of initial investigations of short-range structure within the inorganic oxide phase using IR and NMR spectroscopies.

[SiO_2–TiO_2]/Nafion Nanocomposites. Ti/Si elemental ratio profiles across the thickness direction are symmetrical about the film center plane and greatest in the near-surface regions. Ti/S elemental ratio profiles show that there is more absolute TiO_2 near the surface than at any other location, especially the middle. We attribute the large TiO_2 concentration in the immediate subsurface regions to the high TBT sol–gel reaction rate compared to the rate of inward TBT diffusion and to the slow TEOS sol–gel reaction rate.

A pure SiO_2-containing PFSI, subjected to stress vs strain analysis, displayed ductility, reflecting that the filler was beneath the percolation threshold. In contrast, mixed incorporation of TiO_2, at the same level, renders the material comparatively brittle, suggesting significant interconnection of the inorganic nanoparticles. Elongation-to-break remains the same for all mixed compositions, and tensile strength increases with increasing Ti/Si ratio. Given that the TiO_2 is overwhelmingly incorporated near the surface, we conclude that this glassy zone controls the mechanical properties of these nanocomposites. Regarding small deformations, it appears on inspection that all samples have essentially the same tensile modulus.

[SiO_2–Al_2O_3]/Nafion Nanocomposites. Al/Si elemental ratio profiles were relatively uniform across film thicknesses, in sharp contrast with profiles for [TiO_2–SiO_2]/Nafion hybrids. Al, in an absolute sense, is rather homogeneously distributed across the thickness direction. ATB and its hydrolyzed forms seem to penetrate deep into the film before polymerizing at a fixed site. Considering the rapid reaction of ATB, one logical explanation of this phenomenon may reside in a high diffusivity for this alkoxide within the PFSI morphology.

Stress vs strain curves for all [SiO_2–Al_2O_3]/Nafion hybrids portray ductility but less elongation-to-break than pure SiO_2-filled Nafion of the same filler level. Perhaps the relatively homogeneous distribution of the SiO_2–Al_2O_3 phase is a condition under which its percolation is impossible throughout any region of the film; in particular, glassy near-surface layers do not exist and the ductile PFSI matrix is always the load-bearing phase for these formulations. Except for the hybrid having the lowest ratio, tensile strength decreases while elongation-to-break remains approximately the same with increasing $(Al/Si)_{average}$.

All hybrids have approximately the same tensile modulus. One might ask, within the context of conventional composite theory, why is this parameter insensitive to inorganic composition? Poor bonding between the phases, as suggested in review of this article, is a reasonable proposition. On the other hand, the fact that tensile strength, as well as elongation-to-break, is profoundly influenced by inorganic composition must be accounted for as well. While the hybrids have different metal/Si ratios, they all have approximately the same overall inorganic content. Conceivably, although unproven, hybrids of equal content, irrespective of composition, might have equal interfacial surface areas to largely account for equal moduli. In the case of Al_2O_3–SiO_2-filled systems, wherein the inorganic phase is most likely noncontiguous, increase in strength would have to be due to strong interactions across particle/polymer interfaces. Perhaps long-range PFSI molecular motions that are significant at high deformations, rather than short-ranged motions responding to small deformations, most strongly influence mechanical tensile properties.

FT-IR spectral subtractions uncovered major peaks characteristic of molecular groups in the SiO_2–Al_2O_3 phase. There appears to be an increase of Si–O–Si groups in loops, as opposed to linear fragments, with increase in $(Al/Si)_{average}$. Evidence of unreacted SiOH groups and Al–O–Si linkages was seen, and considerable distortion from coordinative symmetry of bonding about SiO_4 tetrahedra within the gel network was inferred from the spectra.

A ^{29}Si solid-state NMR study of a $SiAl_2O_5$ (6.5%, Al/Si ~ 0.19)/Nafion hybrid contained three peaks corresponding to the following possible coordinations about SiO_4 tetrahedra: (1) $(SiO)_2Si(OH)_2$ and/or $(SiO)Si(OAl)_3$; (2) $(SiO)_3SiOH$ and/or $(SiO)_3SiOAl$; (3) $(SiO)_4Si$. The corresponding IR investigation suggests (1) dominance of the $(SiO)_2Si(OH)_2$ over the $(SiO)Si(OAl)_3$ fragment, and (2) dominance of the $(SiO)_3SiOH$ over the $(SiO)_3SiOAl$ structure, although, pending further studies, much uncertainty remains in these tentative assignments.

^{27}Al NMR spectra would provide complementary information on whether compositional segregation of the sort crudely depicted in Figure 1 occurs. There is presently no information, for example, on the existence of Al–O–Al groups in loops or chains.

Systematic ^{27}Al as well as ^{29}Si NMR studies of samples having various Si/Al ratios is needed to identify Si–O–Al bond formation and sort out topological and compositional aspects of the incorporated inorganic oxide network. These studies will be conducted in the future.

Pending a refined knowledge of these hybrids, to be derived from future studies, a measure of our interpretation of the inorganic oxide phase morphology must be considered speculative, and the tentative interpretations offered are meant to stimulate experimental design. On the other hand, firm facts and strong inferences emerged from these investigations regarding the concentration distribution of the inorganic oxide component across the thickness direction, aspects of inorganic oxide molecular topology (i.e., network coordination states, cyclic vs linear –X–O–X–O– fragments), and the important issue of whether the inorganic phase is contiguous over macroscopic dimensions (i.e., isolated or cocontinuous phases). Moreover, the results from the different characterizations, in large measure, are consistent and complementary, although a number of issues remain unresolved.

In discussing this work dealing with nucleation + growth of very small inorganic oxide particles in a constrained, quasiordered polymer environment (including Teflon-like crystallinity[19]), the topic of *biomimicry* comes to mind. In particular, reproducing the structure,

(19) Starkweather, H. W. *Macromolecules* **1982**, *15*, 320.

and thereby beneficial mechanical properties of bone, as discussed by Burdon et al., is of interest.[20] In bone, nanometers-thick, ribbon-shaped hydroxyapatite crystals intimately incorporated in collagen result in the properties of stiffness, strength, and toughness; high aspect ratio and high packing density are considered to be important in achieving these properties. While high packing density exists for these PFSI-based nanocomposites (internanoparticle spacings ~35 Å[5,6]), high aspect ratio most likely does not, although detailed morphological inquiries of particle shape are clearly needed. On the other hand, it is significant that we have been able, by uniaxial mechanical deformation, to induce anisotropic ionic clusters in unfilled PFSIs[21] as well as to produce oriented SiO_2/PFSI nanocomposite membranes.[10] For the latter, the stress vs strain profile along the draw direction is very different than along the transverse direction and both profiles are different than that for unoriented nanocomposites. It is relevant to this discussion that, in early industrial chloralkali cells, Ca^{2+} and phosphate, existing as hardness factors in brine solutions contacting Nafion membranes, can readily precipitate in the membrane in the form of small strongly incorporated crystals.[22,23] We hesitate to say, however, that the hybrids in our studies represent a model for biomineralization in more than a very general sense.

Finally, we anticipate that the considerable degree of molecular unconnectedness, or "porosity" of the inorganic oxide phase will impart molecular size exclusion for gaseous permeants in these hybrids. This property, coupled with gas molecule interactive selectivity, tortuosity considerations, and the ability to tailor inorganic oxide composition profiles (particularly with regard to asymmetric profiles), suggests that these nanocomposite membranes would be good candidates for gas or perhaps liquid pervaporation separation applications on an industrial scale. We have, in fact, initiated gas permeation investigations of SiO_2/Nafion hybrid membranes and have noted dual-mode sorption behavior.[8,9]

Acknowledgment. This material is based partly upon work supported by a grant from the National Science Foundation/Electric Power Research Institute (Advanced Polymeric Materials, DMR-9211963). This work was also sponsored in part by the Air Force Office of Scientific Research, Air Force Systems Command, USAF, under grant number AFOSR F49620-93-1-0189. The U.S. Government is authorized to reproduce and distribute reprints for Governmental purposes notwithstanding any copyright notation thereon. We acknowledge the assistance of W. Jarrett, Department of Polymer Science, University of Southern Mississippi, in obtaining the ^{29}Si solid-state NMR spectra. The donation of Nafion membranes by the E. I. duPont de Nemours & Co., through the efforts of J. T. Keating, is appreciated, as well. Finally, we respectfully dedicate this paper to the memory of Dr. Phoebe L. Shao.

CM940365G

(20) Burdon, J.; Szmania, J.; Calvert, P. In *Molecularly Designed Ultrafine/Nanostructured Materials*; Gonsalves, K. E., Chow, G.-M., Xiao, T. D., Cammarata, R. C., Eds.; *Mater. Res. Soc. Symp. Proc.* **1994**, *351*, 103.

(21) Cable, K. M.; Mauritz, K. A.; Moore, R. B. *Am. Chem. Soc., Polym. Prepr.* **1994**, *35* (2), 854.

(22) Maloney, D. E.; Molnar, C. J. Membrane Performance in Electrochemical Environment; E. I. DuPont de Nemours & Co., commercial product literature.

(23) Molnar, C. J.; Dorio, M. M. *Electrochem. Soc. Extended Abstr.* **1977**, *77* (2), 1147.